Low-Lying Collective Levels in $^{224\text{-}234}$Th Nuclei

Sohair M. Diab

Faculty of Education, Phys. Dept., Ain Shams University, Cairo, Egypt

E-mail: mppe2@yahoo.co.uk

The low-lying collective levels in $^{224\text{-}234}$Th isotopes are investigated in the frame work of the interacting boson approximation model (IBA-1). The contour plot of the potential energy surfaces, $V(\beta,\gamma)$, shows two wells on the prolate and oblate sides which indicate that all thorium nuclei are deformed and have rotational characters. The levels energy, electromagnetic transition rates B(E1) and B(E2) are calculated. Bending at angular momentum $I^+ = 20$ has been observed for ^{230}Th. Staggering effect has been calculated and beat patterns are obtained which indicate the existence of an interaction between the ground state band, (GSB), and the octupole negative parity band, (NPB). All calculated values are compared with the available experimental data and show reasonable agreement.

1 Introduction

The level schemes of $^{224\text{-}234}$Th isotopes are characterized by the existence of two bands of opposite parity and lie in the region of octupole deformations. The primary evidence for this octupole deformaton comes from the parity-doublet bands, fast electric transition $(E1)$ between the negative and positive parity bands and the low-lying 1^-, 0_2^+ and 2_2^+ excitation energy states. This kind of deformation has offered a real challenge for nuclear structure models. Even-even thorium nuclei have been studied within the frame work of the $Spdf$ interacting boson model [1] and found the properties of the low-lying states can be understood without stable octupole deformation. High spin states in some of these nuclei suggest that octupole deformation develops with increasing spin.

A good description of the first excited positive and negative parity bands of nuclei in the rare earth and the actinide region has achieved [2–4] using the interacting vector boson model. The analysis of the eigen values of the model Hamiltonian reveals the presence of an interaction between these bands. Due to this interaction staggering effect has reproduced including the beat patterns.

Shanmugam-Kamalahran (SK) model [5] for α-decay has been applied successfully to $^{226\text{-}232}$Th for studying their shapes, deformations of the parent and daughter nuclei as well as the charge distribution process during the decay. Also, a solution of the Bohr Hamiltonian [6] aiming at the description of the transition from axial octupole deformation to octupole vibrations in light actinides ^{224}Ra and ^{226}Th is worked out.The parameter free predictions of the model are in good agreement with the experimental data of the two nuclei, where they known to lie closest to the transition from octupole deformation to octupole vibrations in this region. A new frame-work for comparing fusion probabilities in reactions [7] forming heavy elements, ^{220}Th, eliminates both theoretical and experimental uncertinities, allowing insights into systematic behavior, and revealing previously hidden characteristics in fusion reactions forming heavy elements.

It is found that cluster model [8] succeeded in reproducing satisfactorily the properties of normal deformed ground state and super deformed excited bands [9, 10] in a wide range of even-even nuclei, $222 \leqslant A \geqslant 242$[11]. The calculated spin dependences [12] to the parity splitting and the electric multi pole transition moments are in agreement with the experimental data. Also, a new formula between half-lives, decay energies and microscopic density-dependent cluster model [13] has been used and the half-lives of cluster radioactivity are well reproduced.

A new imperical formula [14], with only three parameters, is proposed for cluster decay half-lives. The parameters of the formula are obtained by making least square fit to the available experimental cluster decay data. The calculated half-lives are compared with the results of the earlier proposed models models, experimental available data and show excellent agreement. A simple description of the cluster decay by suggesting a folding cluster-core interaction based on a self-consistant mean-field model [15]. Cluster decay in even-even nuclei above magic numbers have investigated.

Until now scarce informations are available about the actinide region in general and this is due to the experimental difficulties associated with this mass region. The aim of the present work is to:

(1) calculate the potential energy surfaces, $V(\beta,\gamma)$, and know the type of deformation exists;

(2) calculate levels energy, electromagnetic transition rates $B(E1)$ and $B(E2)$;

(3) study the relation between the angular momentum I, the rotational angular frequency $\hbar\omega$ and see if there any bending for any of thorium isotopes;

(4) calculate staggering effect and beat patterns to study the interaction between the $(+\mathrm{ve})$ and $(-\mathrm{ve})$ parity bands.

nucleus	EPS	$PAIR$	ELL	QQ	OCT	HEX	$E2SD(eb)$	$E2DD(eb)$
^{224}Th	0.2000	0.000	0.0081	−0.0140	0.0000	0.0000	0.2150	−0.6360
^{226}Th	0.2000	0.000	0.0058	−0.0150	0.0000	0.0000	0.2250	−0.6656
^{228}Th	0.2000	0.0000	0.0052	−0.0150	0.0000	0.0000	0.1874	−0.5543
^{230}Th	0.2000	0.0000	0.0055	−0.0150	0.0000	0.0000	0.1874	−0.5543
^{232}Th	0.2000	0.0000	0.0055	−0.0150	0.0000	0.0000	0.1820	−0.5384
^{234}Th	0.2000	0.0000	0.0063	−0.0150	0.0000	0.0000	0.1550	−0.4585

Table 1: Parameters used in IBA-1 Hamiltonian (all in MeV).

2 (IBA-1) model

2.1 Level energies

The IBA-1 model was applied to the positive and negative parity low-lying states in even-even $^{224\text{-}234}$Th isotopes. The proton, π, and neutron, ν, bosons are treated as one boson and the system is considered as an interaction between s-bosons and d-bosons. Creation $(s^{\dagger}d^{\dagger})$ and annihilation $(s\tilde{d})$ operators are for s and d bosons. The Hamiltonian [16] employed for the present calculation is given as:

$$\begin{aligned} H &= EPS \cdot n_d + PAIR \cdot (P \cdot P) \\ &+ \frac{1}{2} ELL \cdot (L \cdot L) + \frac{1}{2} QQ \cdot (Q \cdot Q) \\ &+ 5OCT \cdot (T_3 \cdot T_3) + 5HEX \cdot (T_4 \cdot T_4) , \end{aligned} \tag{1}$$

where

$$P \cdot p = \frac{1}{2} \left[\begin{array}{c} \left\{ (s^{\dagger}s^{\dagger})^{(0)}_0 - \sqrt{5}(d^{\dagger}d^{\dagger})^{(0)}_0 \right\} x \\ \left\{ (ss)^{(0)}_0 - \sqrt{5}(\tilde{d}\tilde{d})^{(0)}_0 \right\} \end{array} \right]^{(0)}_0 , \tag{2}$$

$$L \cdot L = -10\sqrt{3} \left[(d^{\dagger}\tilde{d})^{(1)} x \, (d^{\dagger}\tilde{d})^{(1)} \right]^{(0)}_0 , \tag{3}$$

$$Q \cdot Q = \sqrt{5} \left[\begin{array}{c} \left\{ (S^{\dagger}\tilde{d} + d^{\dagger}s)^{(2)} - \frac{\sqrt{7}}{2} (d^{\dagger}\tilde{d})^{(2)} \right\} x \\ \left\{ (s^{\dagger}\tilde{d} + +\tilde{d}s)^{(2)} - \frac{\sqrt{7}}{2} (d^{\dagger}\tilde{d})^{(2)} \right\} \end{array} \right]^{(0)}_0 , \tag{4}$$

$$T_3 \cdot T_3 = -\sqrt{7} \left[(d^{\dagger}\tilde{d})^{(2)} x \, (d^{\dagger}\tilde{d})^{(2)} \right]^{(0)}_0 , \tag{5}$$

$$T_4 \cdot T_4 = 3 \left[(d^{\dagger}\tilde{d})^{(4)} x \, (d^{\dagger}\tilde{d})^{(4)} \right]^{(0)}_0 . \tag{6}$$

In the previous formulas, n_d is the number of boson; $P \cdot P$, $L \cdot L$, $Q \cdot Q$, $T_3 \cdot T_3$ and $T_4 \cdot T_4$ represent pairing, angular momentum, quadrupole, octupole and hexadecupole interactions between the bosons; EPS is the boson energy; and $PAIR$, ELL, QQ, OCT, HEX is the strengths of the pairing, angular momentum, quadrupole, octupole and hexadecupole interactions.

2.2 Transition rates

The electric quadrupole transition operator [16] employed in this study is given by:

$$\begin{aligned} T^{(E2)} &= E2SD \cdot (s^{\dagger}\tilde{d} + d^{\dagger}s)^{(2)} + \\ &+ \frac{1}{\sqrt{5}} E2DD \cdot (d^{\dagger}\tilde{d})^{(2)} . \end{aligned} \tag{7}$$

The reduced electric quadrupole transition rates between $I_i \to I_f$ states are given by

$$B(E_2, I_i - I_f) = \frac{[< I_f \parallel T^{(E_2)} \parallel I_i >]^2}{2I_i + 1} . \tag{8}$$

3 Results and discussion

3.1 The potential energy surface

The potential energy surfaces [17], $V(\beta, \gamma)$, for thorium isotopes as a function of the deformation parameters β and γ have been calculated using :

$$\begin{aligned} &E_{N_{\Pi} N_{\nu}}(\beta, \gamma) = <N_{\pi} N_{\nu}; \beta\gamma \,|H_{\pi\nu}|\, N_{\pi} N_{\nu}; \beta\gamma> = \\ &= \zeta_d (N_{\nu} N_{\pi}) \beta^2 (1 + \beta^2) + \beta^2 (1 + \beta^2)^{-2} \times \\ &\times \left\{ k N_{\nu} N_{\pi} [4 - (\bar{X}_{\pi} \bar{X}_{\nu}) \beta \cos 3\gamma] \right\} + \\ &+ \left\{ [\bar{X}_{\pi} \bar{X}_{\nu} \beta^2] + N_{\nu} (N_{\nu} - 1) \left(\frac{1}{10} c_0 + \frac{1}{7} c_2 \right) \beta^2 \right\} , \end{aligned} \tag{9}$$

where

$$\bar{X}_{\rho} = \left(\frac{2}{7} \right)^{0.5} X_{\rho} \quad \rho = \pi \text{ or } \upsilon . \tag{10}$$

The calculated potential energy surfaces, $V(\beta, \gamma)$, for thorium series of isotopes are presented in Fig. 1. It shows that all nuclei are deformed and have rotational-like characters. The prolate deformation is deeper than oblate in all nuclei except ^{230}Th.The two wells on both oblate and prolate sides are equals and O(6) characters is expected to the nucleus. The energy and electromagnetic magnetic transition rates ratio are not in favor to that assumption and it is treated as a rotational-like nucleus.

$I_i^+ I_f^+$	^{224}Th	^{226}Th	^{228}Th	^{230}Th	^{232}Th	^{234}Th
0_1 Exp. 2_1	——-	6.85(42)	7.06(24)	8.04(10)	9.28(10)	8.00(70)
0_1 Theor. 2_1	4.1568	6.8647	7.0403	8.038	9.2881	8.0559
2_1 0_1	0.8314	1.3729	1.4081	1.6076	1.8576	1.6112
2_2 0_1	0.0062	0.0001	0.0044	0.0088	0.0105	0.0079
2_2 0_2	0.4890	0.8357	0.8647	1.0278	1.2683	1.1659
2_3 0_1	0.0127	0.0272	0.0211	0.0157	0.0122	0.0075
2_3 0_2	0.1552	0.0437	0.0020	0.0023	0.0088	0.0099
2_3 0_3	0.1102	0.0964	0.0460	0.0203	0.0079	0.0023
2_4 0_3	0.2896	0.4907	0.5147	0.6271	0.8048	0.7786
2_4 0_4	0.1023	0.0709	0.0483	0.0420	0.0385	0.0990
2_2 2_1	0.1837	0.1153	0.0599	0.0387	0.0286	0.0174
2_3 2_1	0.0100	0.0214	0.0211	0.0198	0.0178	0.0118
2_3 2_2	0.8461	1.0683	0.5923	0.2989	0.1538	0.0697
4_1 2_1	1.3733	2.0662	2.0427	2.2957	2.6375	2.2835
4_1 2_2	0.0908	0.1053	0.0764	0.0579	0.0445	0.0266
4_1 2_3	0.0704	0.0325	0.0104	0.0038	0.0018	0.0008
6_1 4_1	1.5696	2.2921	2.2388	2.4979	2.8606	2.4745
6_1 4_2	0.0737	0.0858	0.0685	0.0585	0.0493	0.0312
6_1 4_3	0.0584	0.0404	0.0198	0.0106	0.0061	0.0029
8_1 6_1	1.5896	2.3199	2.2720	2.5381	2.9105	2.5220
8_1 6_2	0.0569	0.0660	0.0554	0.0511	0.0466	0.0314
8_1 6_3	0.0483	0.0421	0.0256	0.0166	0.0109	0.0055
10_1 8_1	1.4784	2.2062	2.1948	2.4760	2.8586	2.4899
10_1 8_2	0.0448	0.0513	0.0438	0.0422	0.0407	0.0290

Table 2: Values of the theoretical reduced transition probability, $B(E2)$ (in $e^2\,b^2$).

$I_i^- I_f^+$	^{224}Th	^{226}Th	^{228}Th	^{230}Th	^{232}Th	^{234}Th
1_1 0_1	0.0428	0.0792	0.1082	0.1362	0.1612	0.1888
1_1 0_2	0.0942	0.0701	0.0583	0.0534	0.0515	0.0495
3_1 2_1	0.1607	0.1928	0.2209	0.2531	0.2836	0.3227
3_1 2_2	0.0733	0.0829	0.0847	0.0817	0.0768	0.0717
3_1 2_3	0.0360	0.0157	0.0054	0.0013	0.0002	0.0000
3_1 4_1	0.0233	0.0441	0.0652	0.0884	0.1150	0.1384
3_1 4_2	0.0170	0.0285	0.0371	0.0424	0.0460	0.0449
5_1 4_1	0.2873	0.3131	0.3363	0.3657	0.3946	——
5_1 4_2	0.0787	0.0834	0.0868	0.0865	0.0835	——
5_1 4_3	0.0160	0.0101	0.0051	0.0020	0.0006	——
7_1 6_1	0.4178	0.4387	0.4581	0.4839	0.5100	——
7_1 6_2	0.0732	0.0757	0.0798	0.0817	0.0812	——
9_1 8_1	0.5532	0.5690	0.5848	0.6070	0.6301	——
9_1 8_2	0.0639	0.0665	0.0707	0.0735	0.0748	——

Table 3: Values of the theoretical reduced transition probability, $B(E1)$ (in $\mu\,e^2 b$).

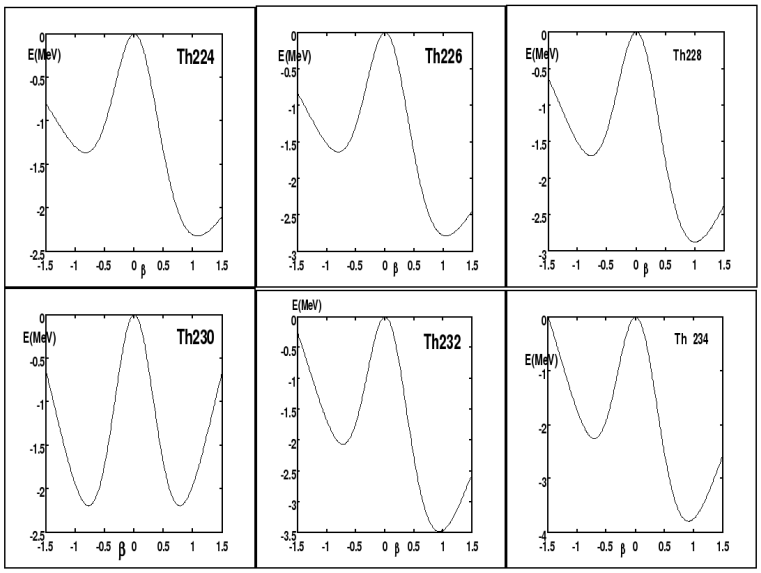

Fig. 1: Potential Energy surfaces for $^{224\text{-}234}$Th nuclei.

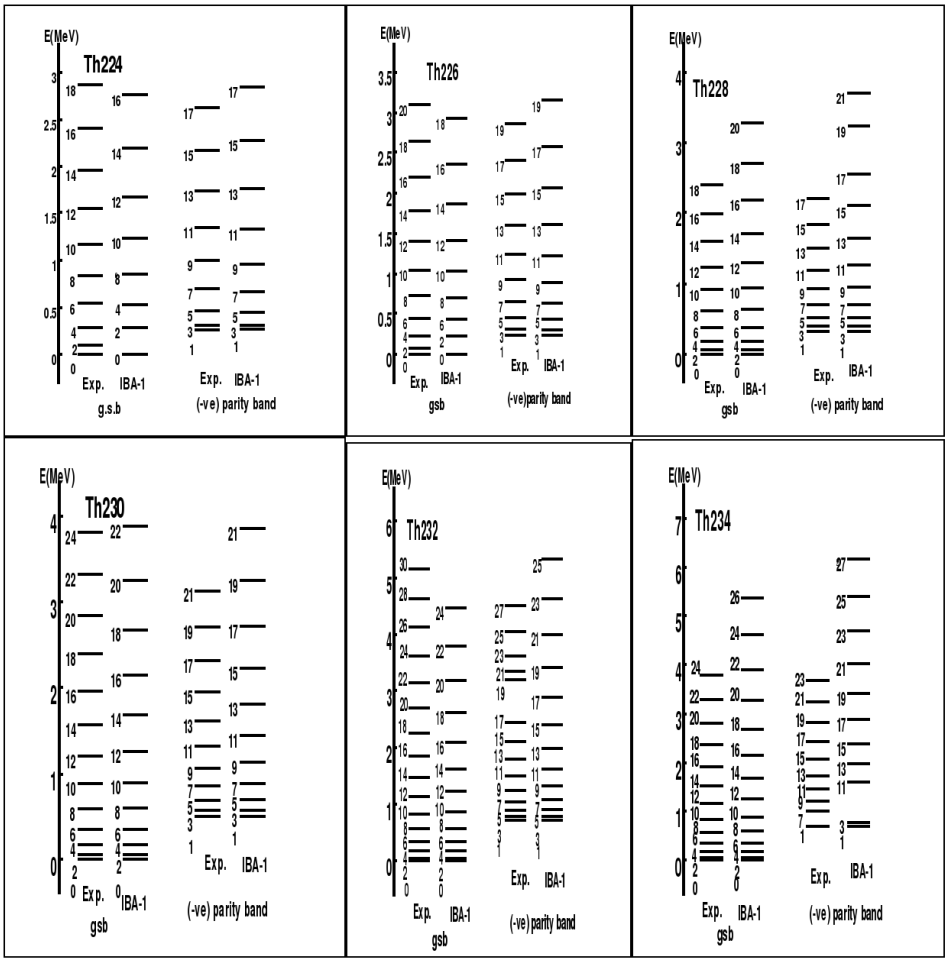

Fig. 2: Comparison between experimental (Exp.) and theoretical (IBA-1) energy levels in $^{224\text{-}234}$Th.

3.2 Energy spectra

IBA-1 model has been used in calculating the energy of the positive and negative parity low -lying levels of thorium series of isotopes. In many deformed actinide nuclei the negative parity bands have been established and these nuclei are considered as an octupole deformed. A simple means to examine the nature of the band is to consider the ratio R which for octupole band , $R \succ 1$, and defined as [18]:

$$R = \frac{E(I+3) - E(I-1)_{NPB}}{E(I) - E(I-2)_{GSB}} . \qquad (11)$$

In the present calculations all values of R for thorium series of isotopes are $\succ$ 1, and we treated them as octupole deformed nuclei.

A comparison between the experimental spectra [19–24] and our calculations, using values of the model parameters given in Table 1 for the ground and octupole bands, are illustrated in Fig. 2. The agreement between the calculated levels energy and their correspondence experimental values for all thorium nuclei are slightly higher especially for the higher excited states. We believe this is due to the change of the projection of the angular momentum which is due to band crossing and octupole deformation.

Unfortunately there is no enough measurements of electromagnetic transition rates $B(E2)$ or $B(E1)$ for these series of nuclei. The only measured $B(E2, 0_1^+ \to 2_1^+)$'s are presented, in Table's 2,3 for comparison with the calculated values. The parameters $E2SD$ and $E2DD$ used in the present calculations are determined by normalizing the calculated values to the experimentally known ones and displayed in Table 1.

For calculating $B(E1)$ and $B(E2)$ electromagnetic transition rates of intraband and interaband we did not introduce any new parameters. Some of the calculated values are presented in Fig. 3 and show bending at $N = 136$, 142 which means there is an interaction between the $(+ve)GSB$ and $(-ve)$ parity octupole bands.

The moment of inertia I and energy parameters $\hbar\omega$ are calculated using equations (12, 13):

$$\frac{2I}{\hbar^2} = \frac{4I - 2}{\Delta E(I \to I-2)} , \qquad (12)$$

$$(\hbar\omega)^2 = (I^2 - I + 1)\left[\frac{\Delta E(I \to I-2)}{(2I-1)}\right]^2 . \qquad (13)$$

All the plots in Fig. 4 show back bending at angular momentum $I^+ = 20$ for ^{230}Th. It means, there is a band crossing and this is confirmed by calculating staggering effect to these series of thorium nuclei. A disturbance of the regular band structure has observed not only in the moment of inertia but also in the decay properties.

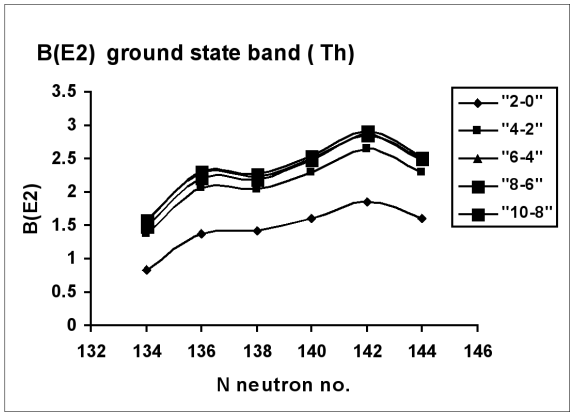

Fig. 3: The calculated $B(E2)$'s for the ground state band of $^{224\text{-}234}$Th isotopes.

3.3 The staggering

The presence of odd-even parity states has encouraged us to study staggering effect for $^{218\text{-}230}$Th series of isotopes [10, 12, 25, 26]. Staggering patterns between the energies of the GSB and the $(-ve)$ parity octupole band have been calculated, $\Delta I = 1$, using staggering function equations (14, 15) with the help of the available experimental data [19–24].

$$Stag(I) = 6\Delta E(I) - 4\Delta E(I-1) - 4\Delta E(I+1) + \Delta E(I+2) + \Delta E(I-2) , \qquad (14)$$

with

$$\Delta E(I) = E(I+1) - E(I) . \qquad (15)$$

The calculated staggering patterns are illustrated in Fig. 5, where we can see the beat patterns of the staggering behavior which show an interaction between the ground state and the octupole bands.

3.4 Conclusions

The IBA-1 model has been applied successfully to $^{224\text{-}234}$Th isotopes and we have got:

1. The ground state and octupole bands are successfully reproduced;
2. The potential energy surfaces are calculated and show rotational behavior to $^{224\text{-}234}$Th isotopes where they are mainly prolate deformed nuclei;
3. Electromagnetic transition rates $B(E1)$ and $B(E2)$ are calculated;
4. Bending for ^{230}Th has been observed at angular momentum $I^+ = 20$;
5. Staggering effect has been calculated and beat patterns are obtained which show an interaction between the ground state and octupole bands;

Submitted on February 09, 2008
Accepted on February 13, 2008

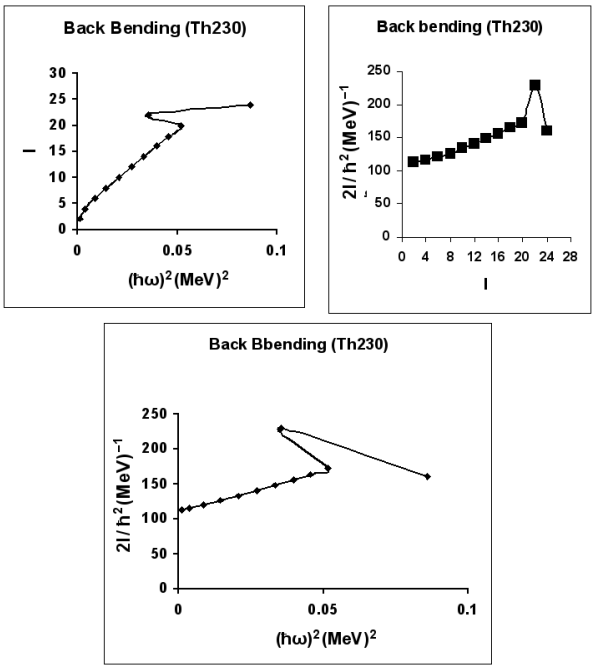

Fig. 4: Angular momentum I as a function of the rotational frequency $(\hbar\omega)^2$ and $2I/\hbar^2$ as a function of $(\hbar\omega)^2$ for the GSB of ^{230}Th.

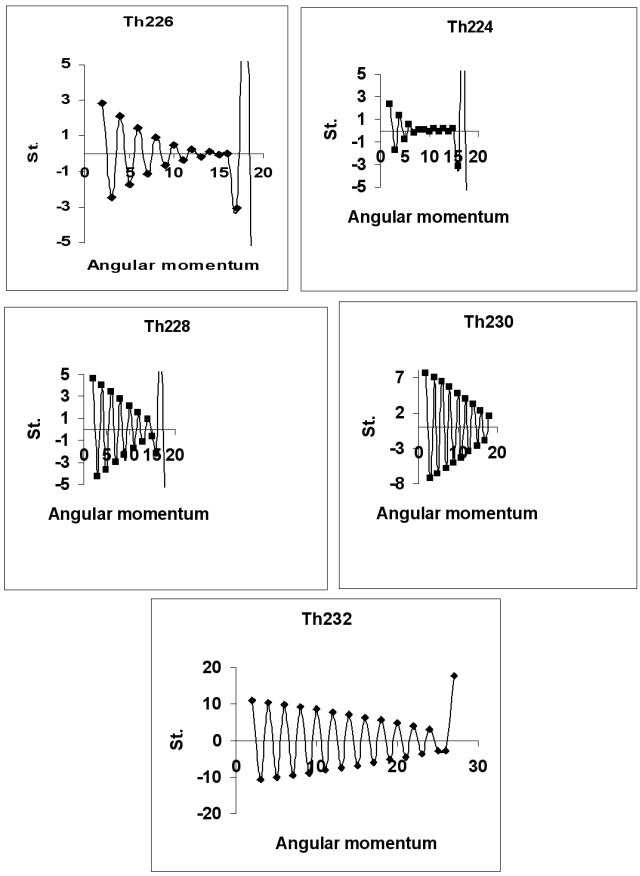

Fig. 5: $\Delta I = 1$, staggering patterns for the ground state and octupole bands of $^{224\text{-}232}$Th isotope.

References

1. Hinde D. J and Dasgupta M.*Nucl. Phys. A*, 2007, v. 787, 176c.
2. Lenis D. and Bonatsos D. *Phys. Lett. B*, 2006, v. 633, 474.
3. Xu F. R. and Pei J. C. *Phys. Lett. B*, 2006, v. 642, 322.
4. Ghanmugam G., Sudhakar S and Niranjani S.*Phys. Rev. C*, 2005, v. 72, 034310.
5. Buck B., Merchant A. C., Perez S. M. and Seals H. E. *J. Phys. G*, 2005, v. 31, 1499.
6. Balasubramaniam M., Kumarasamy S. and Arunachalam N. *Phys. Rev. C*, 2004, v. 70, 017301.
7. Zhongzhou Ren, Chang Xu and Zaijun Wang. *Phys. Rev. C*, 2004, v. 70, 034304.
8. Shneidman T. M., Adamian G. G., Antonenko N. V., Jolos R. V. and Scheid W. *Phys. Rev. C*, 2003, v. 67, 014313.
9. Buck B., Merchant A. C. and Perez S. M. *Phys. Rev. C*, 2003, v. 68, 024313.
10. Ganev V. P., Garistov V. P., and Georgieva A. I. *Phys. Rev. C*, 2004, v. 69, 014305.
11. Minkov N., Drenska S. B.,Drenska S. B., Raychev P. P., Roussev R. P. and Bonatsos D. *Phys. Rev. C*, 2001, v. 63, 044305.
12. Bonatsos D., Daskaloyannis C., Drenska S. B., Karoussos N., Minkov N., Raychev P. P. and Roussev R. P. *Phys. Rev. C*, 2000, v. 62, 024301.
13. Adamian G. G., Antonenko N. V., Jolos R. V., Palchikov Yu. V., Scheid W. and Shneidman T. M. *Nucl. Phys. A*, 2004, v. 734, 433.
14. Buck B., Merchant A. C., Horner M. J. and Perez S. M. *Phys. Rev. C*, 2000, v. 61, 024314.
15. Zamfir N. V. and Kusnezov D. *Phys. Rev. C*, 2001, v. 63, 054306.
16. Feshband H. and Iachello F. *Ann. Phys.*, 1974, v. 84, 211.
17. Ginocchio J. N and Kirson M. W. *Nucl. Phys. A*, 1980, v. 350, 31.
18. Gross E., de Boer J., Diamond R.M., Stephens F. S. and Tjom P. *Phys. Rev. Lett*, 1975, v. 35, 565.
19. Agda Artna-Cohen. *Nucl. Data Sheets*, 1997, v. 80, 227.
20. Akovali Y. A. *Nucl. Data Sheets*, 1996, v. 77, 433.
21. Agda Artna-Cohen. *Nucl. Data Sheets*, 1997, v. 80, 723.
22. Akovali Y. A. *Nucl. Data Sheets*, 1993, v. 69, 155.
23. Browne E. *Nucl. Data Sheets*, 2006, v. 107, 2579.
24. Browne E. *Nucl. Data Sheets*, 2007, v. 108, 681.
25. Minkov N., Yotov P., Drenska S. and Scheid W. *J. Phys. G*, 2006, v. 32, 497.
26. Minkov N., Drenska S. B., Raychev P. P., Roussev R. P.and Bonatsos D. *Phys. Rev. C*, 2001, v. 63, 044305.